



# Plastics, Rubber and Composites

## Macromolecular Engineering

ISSN: 1465-8011 (Print) 1743-2898 (Online) Journal homepage: <https://www.tandfonline.com/loi/yprc20>

## Study on micromoulding of a high viewing angle LED lens

Min-Wen Wang, Fatahul Arifin & Hong-Lin Kuo

To cite this article: Min-Wen Wang, Fatahul Arifin & Hong-Lin Kuo (2019): Study on micromoulding of a high viewing angle LED lens, *Plastics, Rubber and Composites*, DOI: [10.1080/14658011.2019.1685803](https://doi.org/10.1080/14658011.2019.1685803)

To link to this article: <https://doi.org/10.1080/14658011.2019.1685803>



Published online: 10 Nov 2019.



Submit your article to this journal [↗](#)



View related articles [↗](#)



View Crossmark data [↗](#)

## Study on micromoulding of a high viewing angle LED lens

Min-Wen Wang<sup>a</sup>, Fatahul Arifin <sup>a,b</sup> and Hong-Lin Kuo<sup>a</sup>

<sup>a</sup>Department of Mechanical Engineering, National Kaohsiung University of Science and Technology, Kaohsiung, Taiwan; <sup>b</sup>Department of Mechanical Engineering, Politeknik Negeri Sriwijaya, Palembang, Indonesia

### ABSTRACT

Lenses are used to mount on the light-emitting diode (LED) chip to obtain the desired light distribution patterns. In this study, a lens for large viewing angle and high uniformity LED has been developed with optical grade poly methyl methacrylate (PMMA) material. TracePro software was used to design the lens while Moldex 3D software was implemented to design the mould and the mould filling phenomena. Together with micromoulding technology and Taguchi experimental method with control parameters were mould temperature (MoT), melt temperature (MT), and injection speed, a lens with optical uniformity of 87.18% and viewing angle of 128° has been developed. The experimental results showed that MoT and MT were the main factors affecting the optical quality, each with contributions greater than 50 and 30%, respectively. Though this lens is relatively small in dimension, a draft angle is needed for successful removal of the moulded PMMA lens from the mould.

### ARTICLE HISTORY

Received 6 May 2019  
Revised 24 September 2019  
Accepted 23 October 2019

### KEYWORDS

Lens; draft angle; LED; lens; micromoulding; Taguchi experimental method; uniformity; viewing angle

### Introduction

Nowadays, science has grown rapidly. Many products are made with sophisticated technologies and with fast and cheap processes. People around the world enjoy these achievements which make their daily life more convenient and comfortable. Due to the invention of light-emitting diodes (LED), coupled with the rising awareness of environmental protection and energy conservation, the optoelectronic industry has provided the new light source that could be the choice of people. LEDs were mostly used as indicators in the early days because of lower power and lack of brightness. However, with the continuous improvement in LED technology, high power, and high luminous LEDs can be seen in the markets.

In 1993, Nichia Corporation launched the first white LED product [1], the luminous efficiency of LEDs has been improved since then, making the LED more widely used in many electronic devices, such as computers, mobile phone monitors, other display backlights, etc. [2].

There are reasons for the fast development of LEDs, such as small in size, lower power consumption, mercury-free, and long life (under normal operating temperature, the theoretical life expectancy of up to 100,000 hours). Besides, countries vigorously promote green lighting programs, and the market demands make the development of LED industries rapidly.

LED lights and LED systems consist of three components: the LED chip, the circuit board, and secondary optics. Secondary optics such as lenses, reflectors, or diffusers are mounted on the circuit board and complete the LED solution [3].

Lenses are often used to mount on the LED chip to obtain the desired light distribution patterns which can be divided into four types of light pattern categories, namely; Batwing, Lambertian, Side-Viewing, and Collimating Optics. The function of the lens is to control the LED crystal to emit light so the LED has different types of light emission. With the advance of optical simulation technologies, computer aided in optical designs have been seen in research and the industries [4]. Chang et al. [5] and Hsu [6] used the optical simulation software such as LightTools and TracePro to determine the LED lens structures and analyse the lenses with the one-factor-one experimental method (OFAT) to find out the best parameters of the lens structures to improve the luminous efficiency and uniformity of LED.

Chen and their laboratory [7] used the optical simulation software TracePro to design the appearance of the LED lens and established the quality predictor of the optical lens with back-propagation neural network to effectively predict the luminescence of the LED optical lens then combined with the genetic algorithm to find the optimal design. The best design of the LED lens has a viewing angle of 135° and the luminous uniformity of 93.35%.

Lo et al. [8] used Advanced Systems Analysis Program to design a butterfly-shaped lens with an unequal tilt design to reduce the size of the dual-LED. The butterfly lens-shaped lens has the optical utilisation factor of 43.8%, the uniformity is 1/2.7, and the averaged illuminance is 141x.

To reduce the absorption of light, the materials for LED lenses usually are high-transmittance optical

**Table 1.** Dimensions of the original design.

A	B	C	D	E	F
0.688	5.024	3.924	2.588	3.0	2.386

plastics. The common optical plastic materials are PMMA, polycarbonate, and cyclic olefin copolymer. LED lenses are usually small in size and with micro features to convert light emitted from the chip to a specially designed pattern. One of the popular manufacturing processes for making micro plastic lenses is micromoulding, it is a fast replication process that can produce parts with small features and complex shapes. Many researchers have used this technology to make lenses in different applications [9–11].

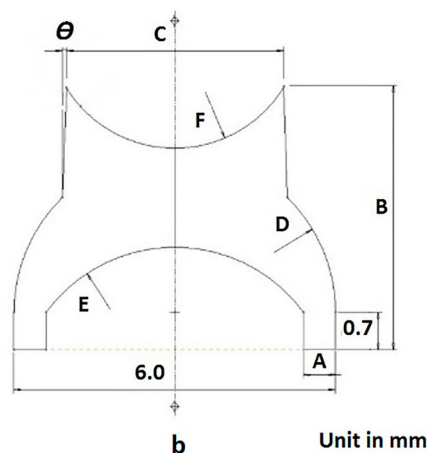
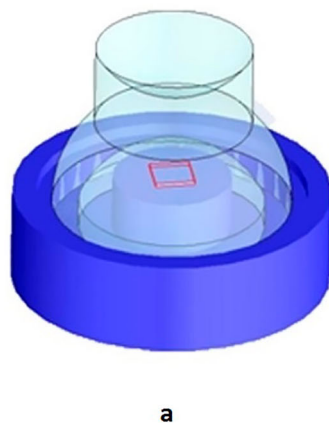
In this study, the high viewing angle lens in reference [7] previously designed by Chen and their laboratory will be developed using micromoulding technology. The moulding draft angle not considered in the original design will be discussed as well as its effect on the lens optical properties. Integrate optical analysis, moulding simulation technology, micromoulding, and Taguchi Experimental method will be carried out in this study to mould the lens with both high luminous and high viewing angle.

## Mould design analysis and injection moulding simulation

### Lens design and optical analysis

The LED lens previously designed is shown in Figure 1 and the dimensions are listed in Table 1. This lens has a viewing angle of  $135^\circ$  and the luminous uniformity of 93.35%. An optical grade PMMA (GH-10008\_1 KUR-ARAY) is selected as the lens material for this study, this PMMA has a transparency of 94% and a refractive index of 1.5. Battenfeld Microsystem 50 micromoulding machine will be utilised to mould this lens.

To successfully remove the moulded lens from the mould, a draft angle along the mould opening direction is considered as shown in Figure 1(b). Figure 2 shows the luminous distributions of the lens when a draft

**Figure 1.** LED lens design and draft angle design location.

angle of  $1^\circ$ ,  $2^\circ$ , and  $3^\circ$  was added to the lens analysed with TracePro optical analysis software.

The luminance uniformity ( $u$ ) is measured by all values of peaks and valleys of the luminous distribution curve, and it can be calculated as follows:

$$\bar{a} = \frac{1}{n} \sum_{i=1}^n a_i \quad (1)$$

$$u = \left( 1 - \frac{\frac{1}{n} \sum_{i=1}^n |a_i - \bar{a}|}{\bar{a}} \right) \times 100\%$$

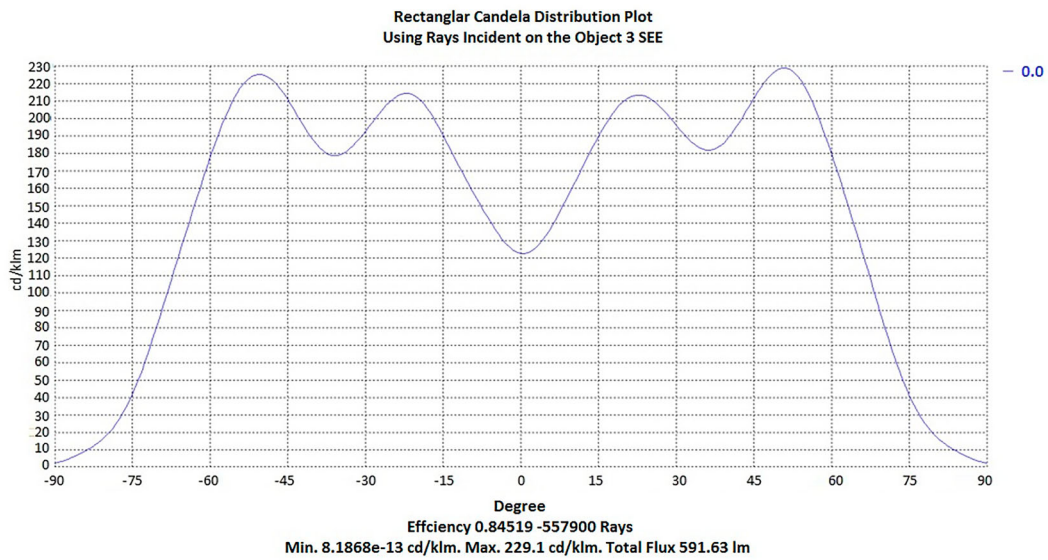
where  $a_i$  are the values of the peaks and valleys in the luminance distribution curve,  $n$  is the total occurrence times of peak and valley of the curves, and  $\bar{a}$  is the mean value of peak and valley [7].

The simulation results showed in Figure 2(a) indicate that the luminous uniformity and the viewing angle for lens with  $1^\circ$  draft angle are 85.03% and  $134^\circ$  and those are 82.64% and  $135^\circ$  for  $2^\circ$  draft angle design (Figure 2(b)), while they are 72.18% and  $136^\circ$  for  $3^\circ$  draft angle design (Figure 2(c)).  $1^\circ$  draft angle is the better design for the lens and will be designed in the mould tool in this study.

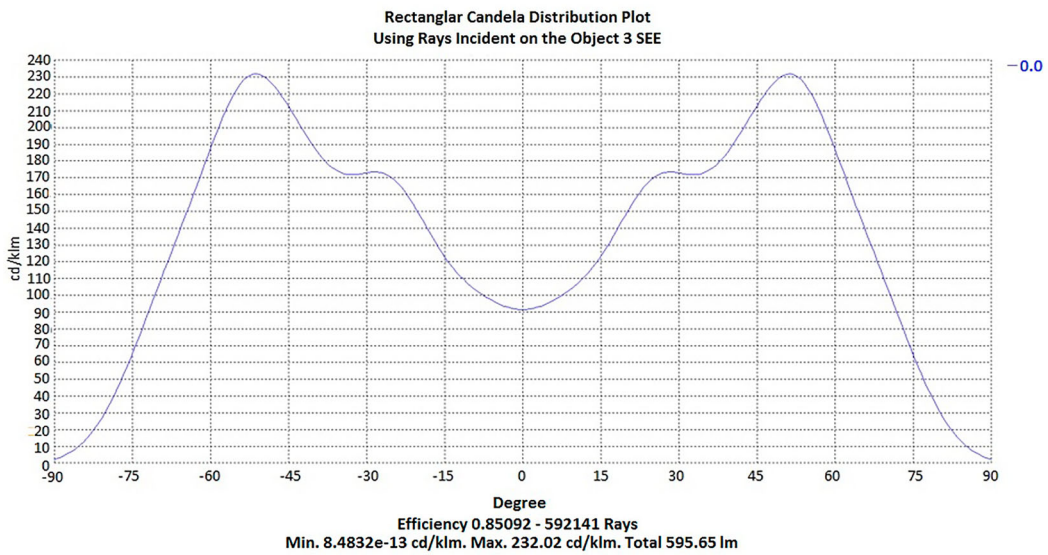
The optical properties were decreased with the extra draft angle design compared to the original design as shown in Figure 2. A redesign lens based on the original design from Chen et al. [7] and with  $1^\circ$  draft angle was developed and shown in Figure 3. The luminous uniformity and the viewing angle for this redesign lens are 88.59% and  $131.28^\circ$  (Figure 4). Though not as good as the original design, its better than those shown in Figure 2. This redesign lens will be used in further moulding experiments in this study.

### Mould design

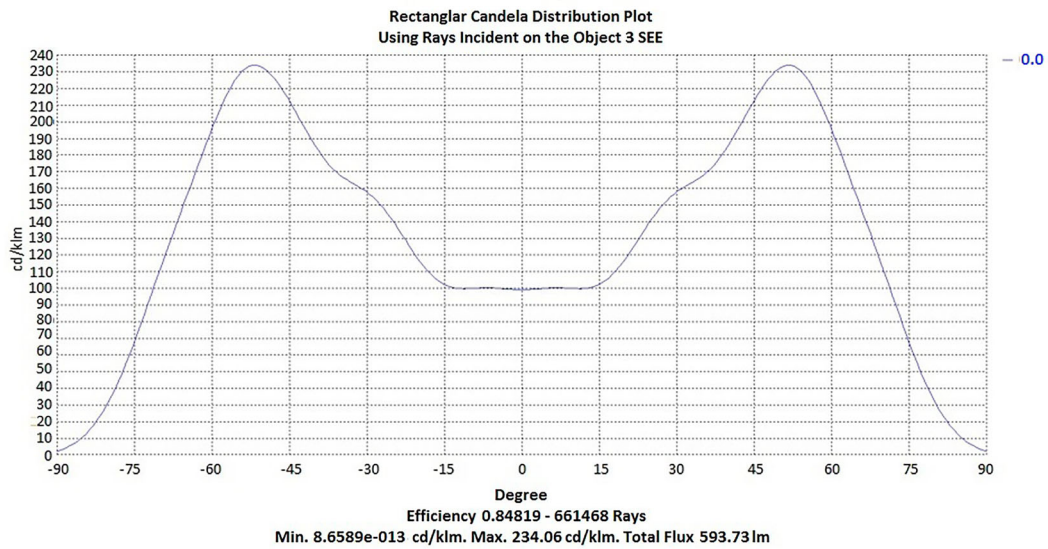
The Battenfeld Microsystems 50 is used for this micromoulding experiment in this study, the sprue and runner system are designed to match the injection unit of this machine as shown in Figure 5.



a. Draft angle 1°



b. Draft angle 2°

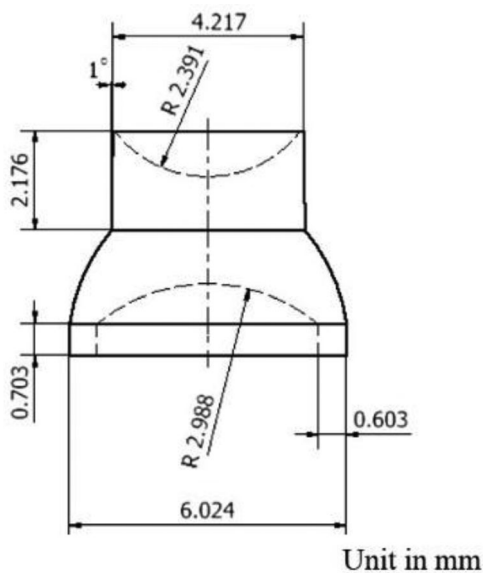


c. Draft angle 3°

**Figure 2.** Luminous distribution analysis with draft angles. (a) Draft angle 1°, (b) Draft angle 2° and (c) Draft angle 3°.

To make this lens using the moulding process, a side gate is selected and the gate position is placed at the lower end edge of the cavity, so it attains to minimise

the effects of performance and appearance of the LED lens. Then, the length, width, and thickness of the gate are 1.5, 1, and 0.6 mm.

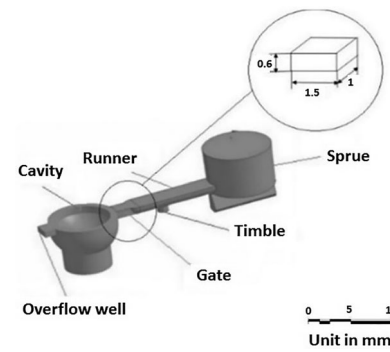


**Figure 3.** Modified lens dimensions.

Mould filling simulation with Moldex3D indicates there are welding lines at the far end of the gate as shown in Figure 6(a). The welding line is one of the defects in plastic injection moulding. Welding lines will cause structural, cosmetic blemishes and surface appearance problems [12–14]. Welding lines should be prevented or minimised in product design, mould design, and processing condition setting. In this study, an overflow well is added at the opposite side of the gate as shown in Figure 5. With this overflow well, the welding lines appear in the well outside the lens instead of inside the lens as shown in Figure 6(b). To successfully eject the part and runner system from the mould after cooling, an eject pin is added as well in the middle of the runner as shown in Figure 6(b).

### Moulding simulation

In this study, Moldex3D was used to analyse the mould filling process. The material for moulding the



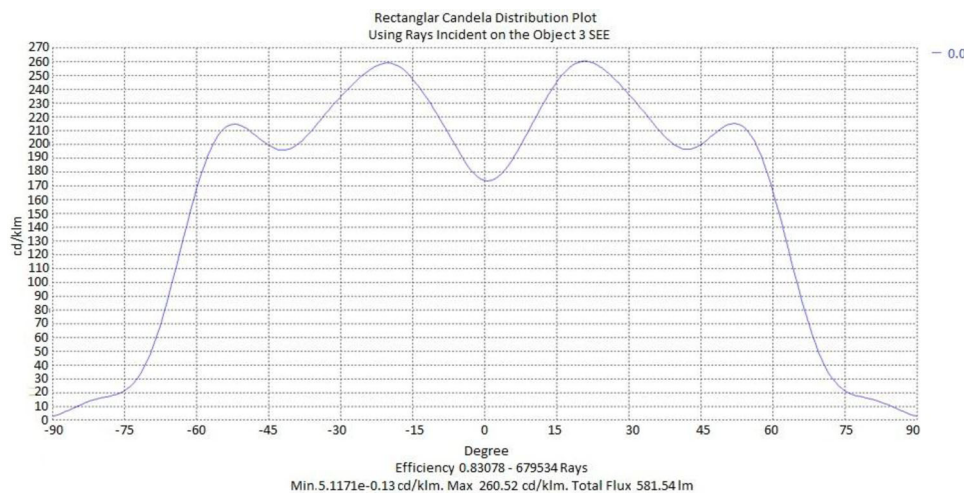
**Figure 5.** Cavity and runner system of the biconcave spherical lens.

biconcave spherical lens is an optical grade PMMA GH-10008\_1 from KURARAY, the recommended processing parameters from the material provider are listed in Table 2.

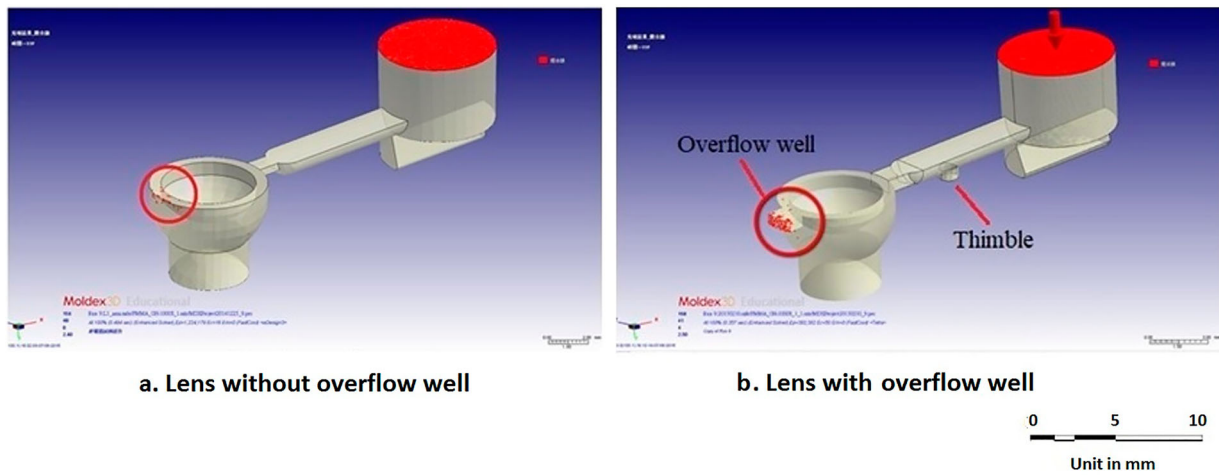
## Parameters design analysis

### Overview of parameters designing process

The Taguchi method is one of the effective ways to find the better processing parameters experimentally, and it will be used in this study to find the best processing parameter combinations and the effects of processing factors on the lens moulding qualities. Oktem et al. [12] used the Taguchi method to minimise product shrinkage and warpage effectively. The results showed that shrinkage and warpage can be significantly improved by about 0.7 and 2.1%. Erzurumlu and Ozcelik [13], Lee and Lin [14] both used the melt temperature (MT), mould temperature (MoT), packing pressure, holding time, and cooling time as the control factors in their studies. In designing the polypropylene plastic shell moulds for casting the HEMA (Hydroxyethyl methacrylate) contact lens, Chen et al. [15] applied the Taguchi method and Moldex3D to analyse the shrinkage of the shell mould. The shrinkage results



**Figure 4.** Light distribution analysis of the redesign lens with 1° draft angle.



**Figure 6.** Welding line locations of the lens.

**Table 2.** PMMA GH-10008\_1 KURARAY processing parameters.

Item	GH-10005
Drying temp. (°C)	80–100
Drying condition (hours)	4–6
MoT. (°C)	50–90
MT (°C)	230–280
Injection pressure (MPa)	80–140

of the simulation were then used to compensate the mould profile to reduce the shrinkage of the shell moulds in the injection moulding process. The simulation result after compensation of the mould shows that the shrinkage error is reduced as 80.8%. The Taguchi method and mould filling simulation technologies are very helpful in the injection moulding process, both will be implemented in this study to find the best processing parameters and mould design.

### Designing the processing window

Before performing the injection moulding simulation process, the processing parameters of the selected material should be set first, then determine the ranges and levels of the control factors for the Taguchi experiments.

For the bi-concave spherical structure lens to function properly, the moulded lens should have a good form of accuracy. Warpage and shrinkage are the two main reasons affecting the moulding part accuracy. Proper MoT can minimise shrinkage and the moulded-in residual stress in the polymer lens production [15]. Higher MoT can lessen the rapid cooling effects of polymer melt inside the mould cavity. Hence, the moulded lenses can be packed better to have higher form accuracy lens production [16]. MT is a valuable factor that impacts on the shrinkage of the lens [17]. Higher the MT, the higher the shrinkage when it was cooled down, but it also provides effective packing that minimises shrinkage. Packing pressure is applied after the filling process and before the melt in the gate is frozen to compensate the melt shrink. Packing

is important especially for non-uniform thickness part like the bi-concave spherical structure lens studied in this paper, it is critical to achieve high accuracy lens production [18].

Among those moulding parameters, MoT, MT, and injection speed (IS), each has a significant influence on the part warpage and shrinkage qualities, thus these were selected as control parameters in the Taguchi experiment in this study.

### Short shot simulation and actual experiment

#### Short shot simulation experiment








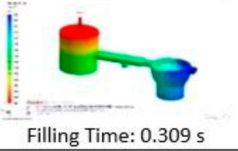








The purpose of the short shot simulation experiment is to find out whether the simulation analysis conditions are consistent with the actual experiment and to observe the plastic filling flow process and the possible moulding defects.

The short shot experiment is done by adjusting the shot volume and to observe the flow of molten material during the injection to the mould cavity and to understand the cause of the formation of the product defects. The simulation with different filling time (20, 40 and 60 mm s<sup>-1</sup>) and actual experiment results are shown in Figure 7.

From Figure 7, we can find that filling pattern between short shot simulation and experiment are similar. When it is filled with 78% volume, the molten material starts to flow into the part through the gate.

#### The control factors

There were many factors is attained affect the product in injection moulding such as MoT, MT, packing pressure, injection pressure, IS, holding time, and cooling time according to previous studies [12–15]. Lee and Lin showed that the shrinkage of the LED product was influenced by MT and MoT [14]. Oktem et al. results indicated IS had a significant impact on the shrinkage and warpage of a multi thin wall tube product was given by IS [12]. The MT, the MoT, and the IS are important factors influencing thin and small part's

Filling (%)	67 %	78 %	93 %	100 %
Simulation Result Injection Speed 20 (mm/s)	 Filling Time: 0.441 s	 Filling Time: 0.541 s	 Filling Time: 0.613 s	 Filling Time: 0.659 s
Simulation Result Injection Speed 40 (mm/s)	 Filling Time: 0.207 s	 Filling Time: 0.241 s	 Filling Time: 0.287 s	 Filling Time: 0.309 s
Simulation Result Injection Speed 60 (mm/s)	 Filling Time: 0.138 s	 Filling Time: 0.160 s	 Filling Time: 0.191 s	 Filling Time: 0.205 s
Actual Result Injection Speed 20				

**Figure 7.** Comparison of the results of simulation and actual experiment.

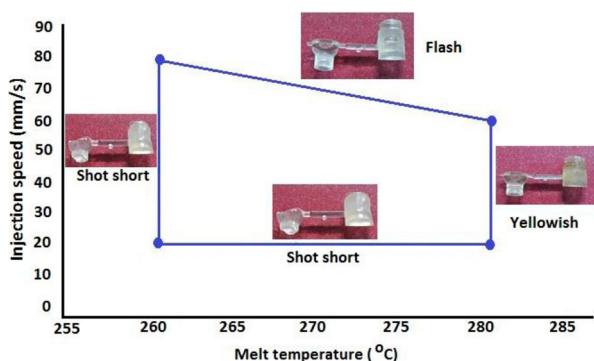
shrinkage and warpage and they are chosen as the control factors in this study as well.

Before the Taguchi experiments, the levels of the selected control factors must be decided first. Table 2 shows the moulding processing ranges of different parameters for this PMMA Kuraray suggested by the material provider.

The results of the processing window experiment can be seen in Figure 8.

For the IS, a short shot occurs when it is lower than  $20 \text{ mm s}^{-1}$ , while overflow happens when it is higher than  $60 \text{ mm s}^{-1}$ . So, the IS range is set  $20\text{--}60 \text{ mm s}^{-1}$ . For the MT, a short shot occurs when it is lower than  $260^\circ\text{C}$ , while burned part happens when it is higher than  $280^\circ\text{C}$ . So, the MT range is set between  $260$  and  $280^\circ\text{C}$ . For the MoT, a short shot occurs when it is lower than  $70^\circ\text{C}$ , while the part and  $90^\circ\text{C}$  is the highest MoT suggested by the supplier. So, the MoT range is set between  $70$  and  $90^\circ\text{C}$  for the Taguchi experiment.

For this Taguchi experiment, three control factors are selected, namely, MoT, MT, and IS. Each of the control factors were assigned with three levels as



**Figure 8.** Processing window of lens moulding.

**Table 3.** The levels of the control factors.

	MoT ( $^\circ\text{C}$ )	MeT ( $^\circ\text{C}$ )	IS ( $\text{mm s}^{-1}$ )
Level 1	70	260	20
Level 2	80	270	40
Level 3	90	280	60

shown in Table 3. Taguchi experiment with an  $L_9(3^3)$  orthogonal array is suitable for this experiment and is shown in Table 4.

The processing parameters kept fixed in the experiments are shot volume ( $270 \text{ mm}^3$ ), screw speed ( $80 \text{ mm s}^{-1}$ ), back pressure ( $80 \text{ bar}$ ), and cooling time ( $15 \text{ seconds}$ ). Before the Taguchi experiment, simulation with Moldex3D indicated the gate was frozen after 1.2 seconds packing as shown in Figure 9, so the packing time was set at 1.5 seconds to ensure enough packing in the moulding experiments. As for the packing pressure, a Moldex3d simulation-based Taguchi experiment has been carried out before the moulding Taguchi experiment as well, and the results showed that  $20 \text{ MPa}$  is a preferred packing pressure for both low shrinkage and low birefringence. For the Battenfeld Microsystem 50, the packing was done through the push speed of the

**Table 4.**  $L_9(3^3)$  Taguchi experiment layout.

Exp.	MoT ( $^\circ\text{C}$ )	MeT ( $^\circ\text{C}$ )	IS ( $\text{mm s}^{-1}$ )
1	70	260	20
2	70	270	40
3	70	280	60
4	80	280	40
5	80	270	60
6	80	260	20
7	90	270	60
8	90	280	20
9	90	260	40

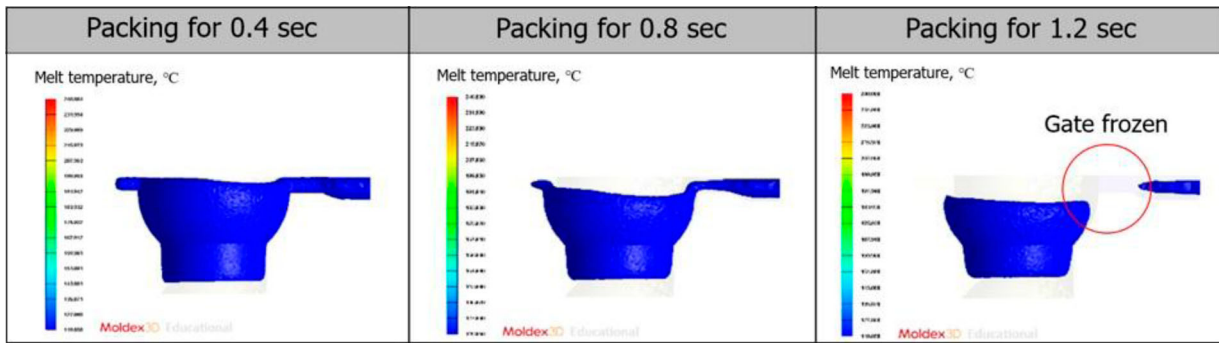


Figure 9. The gate condition after packing.

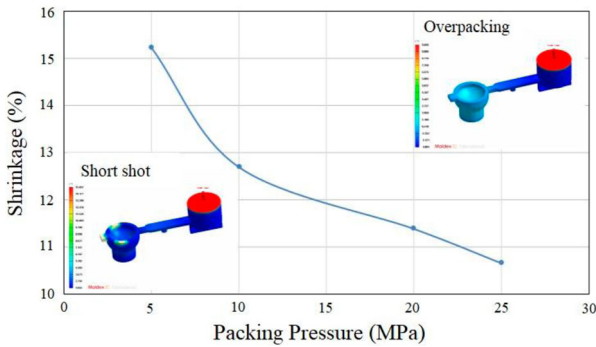


Figure 10. Simulation result shrinkage versus packing pressure.

injection piston, and the range is  $0\text{--}33\text{ mm s}^{-1}$  since  $20\text{ MPa}$  is not a very high packing pressure, so the packing speed was set at  $10\text{ mm s}^{-1}$  in the Taguchi experiments. Simulation results also indicate that shrinkage decreases when packing pressure increases (Figure 10). However, there will be overpacking when the pressure reaches  $25\text{ MPa}$ .

## Results and discussion

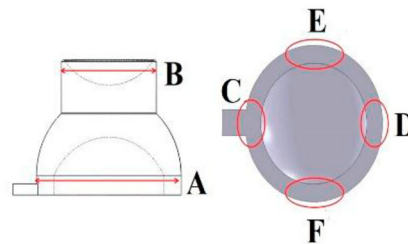
### The Taguchi method experimental results

The primary purpose of this experiment is to observe the feasibility of moulding the biconcave spherical structure

lens with a substantial difference in thickness ratio and sharp edge and find the effects of moulding parameters on the moulding quality. The finished parts should be defect-free, and the dimensions should be close to the original design. Moulded part shrinkage was selected as the quality index for this Taguchi experiment.

The moulded lenses were shown in Figure 11 After moulding, the parts will sit for 24 hours before the dimension measurement.

Three parts for each experimental run will be selected randomly and measured. Dimensions at six different locations of the part shown in Figure 12 will



- Remarks :
- A. Top circle diameter
  - B. Bottom circle diameter
  - C. The bottom circle inside and outside the diameter difference (near the gate)
  - D. The bottom circle inside and outside the diameter difference (far the gate)
  - E. The bottom circle inside and outside the diameter difference (front)
  - F. The bottom circle inside and outside the diameter difference (back)

Figure 12. The measurement area of the LED lens.

	Top View	Bottom view	Side view
Lens and runner system			
Lens			

Figure 11. Product feature.



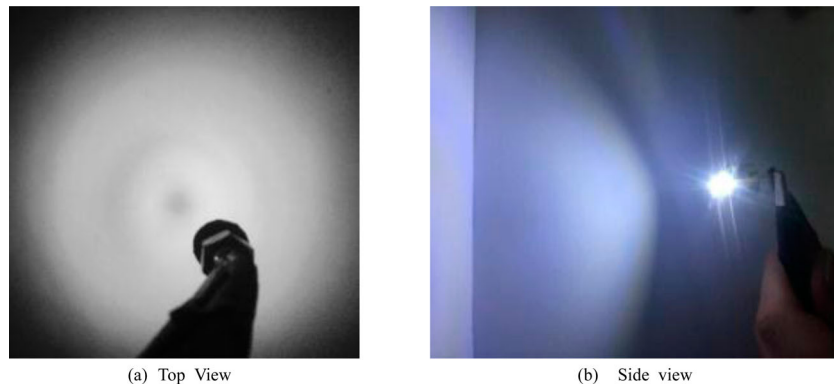


Figure 13. Actual illumination.

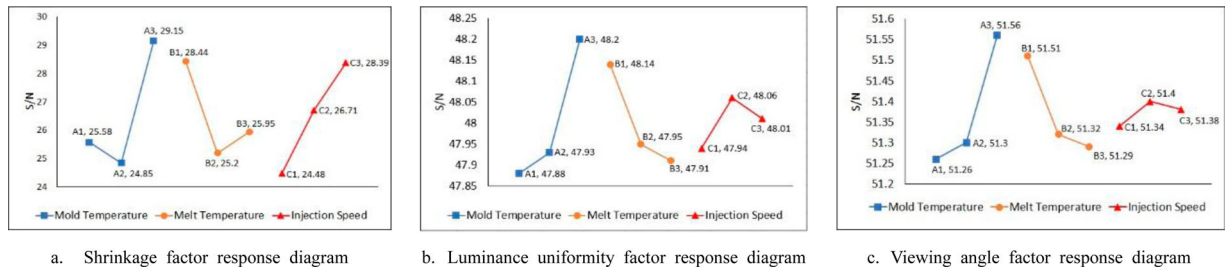


Figure 14. The response diagram of Taguchi experiment of LED.

be measured. The linear shrinkage  $L_S$  of each dimension can be calculated by the following equation

$$L_S = \left[ \frac{\text{Part}_{\text{size}} - \text{Mould}_{\text{size}}}{\text{Mould}_{\text{size}}} \right] \times 100\% \quad (2)$$

where  $\text{Mould}_{\text{size}}$  is the mould dimension and  $\text{Part}_{\text{size}}$  is the dimension measured from the moulded part. The  $\text{Mould}_{\text{size}}$  dimensions to be measured are shown in Figure 3, where  $A$  is 4.217 mm,  $B$  is 6.024 mm,  $C$  is 0.703 mm,  $D$  is 0.703 mm,  $E$  is 0.703 mm, and  $F$  is 0.703 mm. Each part has six linear shrinkage numbers, and the average of these represents the linear shrinkage of the part. The averaged linear shrinkage of the measurements will be calculated and represent the quality of the part ( $y$ ).

The part is expected to shrink as small as possible, so it is smaller-the-better experiment. The S/N ratio of the

smaller-the-better characteristic will be calculated using Equation (3) in this experiment [19].

$$\eta_{\text{STB}} = -10 \log \left( \frac{1}{n} \sum_{i=1}^n y_i^2 \right) \quad (3)$$

where  $y_i$  is the average volume shrinkage,  $n$  is the number of samples.

Figure 13 shows the actual illumination with the lens assembled with the LED. The luminance distribution of the lens is measured with a Goniophotometer (type HLED-Gonio 8). The luminance uniformity and the viewing angle of the lens are expected to be as large as possible, so these are larger the better experiments. The S/N ratio of the larger-the-better characteristic will be calculated using Equation (4) in these two

Table 5. The results of the shrinkage Taguchi experiment.

Exp.	MoT (°C)	MeT (°C)	IS (mm s <sup>-1</sup> )	Shrinkage (%)			Average shrinkage (%)	S/N
				$y_1$	$y_2$	$y_3$		
1	70	260	20	4.984	4.806	4.859	4.883	26.076
2	70	270	40	6.571	6.197	6.464	6.411	23.484
3	70	280	60	4.431	4.824	4.663	4.639	25.943
4	80	280	40	5.59	5.43	5.394	5.471	25.082
5	80	260	60	3.914	3.843	4.128	3.962	27.469
6	80	270	20	8.515	8.783	8.604	8.634	21.168
7	90	270	60	3.058	3.111	2.826	2.998	29.468
8	90	280	20	4.966	5.162	5.002	5.043	25.762
9	90	260	40	2.755	2.969	2.684	2.803	29.969
			Sample		1	2	3	Average
Optimal	90	260	60	Shrinkage (%)	2.264	2.269	2.268	2.267
				Luminance uniformity (%)	86.41	86.50	86.49	86.471
				Viewing angle (°)	125	127	127	126.3

**Table 6.** The results of the luminance uniformity Taguchi experiment.

Exp.	MoT (°C)	MeT (°C)	IS (mm s <sup>-1</sup> )	Luminance uniformity (%)			Average luminance uniformity (%)	S/N
				y <sub>1</sub>	y <sub>2</sub>	y <sub>3</sub>		
1	70	260	20	83.69	83.77	83.34	83.600	47.99
2	70	270	40	82.89	83.01	82.76	82.887	47.91
3	70	280	60	81.24	81.05	81.33	81.207	47.73
4	80	280	40	83.17	83.1	82.97	83.080	47.93
5	80	260	60	84.67	84.55	84.87	84.697	48.10
6	80	270	20	81.51	81.47	81.44	81.473	47.76
7	90	270	60	85.54	85.66	85.45	85.550	48.19
8	90	280	20	84.43	84.56	84.32	84.437	48.07
9	90	260	40	87.21	87.03	86.95	87.063	48.34
			Sample		1	2	3	Average
Optimal	90	260	40	Shrinkage (%)	2.769	2.785	2.809	2.789
				Luminance uniformity (%)	87.29	87.34	86.96	87.182
				Viewing angle (°)	127	128	129	128

**Table 7.** The results of the viewing angle Taguchi experiment.

Exp.	MoT (°C)	MeT (°C)	IS (mm s <sup>-1</sup> )	Viewing angle (°)			Average viewing angle (°)	S/N
				y <sub>1</sub>	y <sub>2</sub>	y <sub>3</sub>		
1	70	260	20	125	124	122	123.667	51.39
2	70	270	40	122	120	122	121.333	51.22
3	70	280	60	120	121	121	120.667	51.17
4	80	280	40	123	122	121	122.000	51.27
5	80	260	60	125	123	125	124.333	51.43
6	80	270	20	121	120	122	121.000	51.20
7	90	270	60	126	125	126	125.667	51.53
8	90	280	20	124	124	125	124.333	51.43
9	90	260	40	128	128	129	128.333	51.71
			Sample		1	2	3	Average
Optimal	90	260	40	Shrinkage (%)	2.769	2.785	2.809	2.789
				Luminance uniformity (%)	87.29	87.34	86.96	87.182
				Viewing angle (°)	127	128	129	128

experiments [19]

$$\eta_{LTB} = -10 \log \left( \frac{1}{n} \sum_{i=1}^n \frac{1}{y_i^2} \right) \quad (4)$$

where  $y_i$  is the average luminance uniformity or viewing angle and  $n$  is the number of samples

**Qualities and parameters**

After the Taguchi experiment, the dimensions of nine groups of products were measured to determine the shrinkage rate of each group. The best combination of the lens shrinkage is A3B1C3 (Figure 14(a)), the best combination of the LED luminance uniformity is A3B1C2 (Figure 14(b)), and finally, it is shown that the best combination of the LED viewing angle is A3B1C2 (Figure 14(c)) as well (Tables 5–7).

**Table 8.** The shrinkage variation analysis.

Factor	Sum of squares (SS)	fDOF (f)	V variation	S' pure change	$\rho$ contribution (%)
MoT	25.449	2	12.724	25.449	42.058
MeT	15.624	2	7.812	15.624	25.820
IS	16.326	2	8.163	16.326	26.981
MoT/MeT	0.914	4	0.229	0.914	1.511
MoT/IS	0.470	4	0.117	0.470	0.776
MeT/IS	0.012	4	0.003	0.012	0.020
MoT/MeT/IS	0.0782	6	0.130	0.782	1.293
Error	0.933				1.541
Total (St)	60.509	24	2.521	60.509	100.00%

**Table 9.** The luminance uniformity variation analysis.

Factor	Sum of squares (SS)	fDOF (f)	V Variation	S' Pure Change	$\rho$ contribution (%)
MoT	0.178	2	0.089	0.178	58.326
MeT	0.090	2	0.045	0.090	29.589
IS	0.022	2	0.011	0.022	7.100
MoT/MeT	0.00420	4	0.00105	0.00420	1.378
MoT/IS	0.00290	4	0.00073	0.00290	0.952
MeT/IS	0.00210	4	0.00053	0.00210	0.689
MoT/MeT/IS	0.00230	6	0.00038	0.00230	0.755
Error	0.00369				1.211
Total (St)	0.30474	24	0.01270	0.30474	100.00%

The experimental results for shrinkage were listed in Table 5, while the variation analysis results were listed in Table 8. It shows that MoT is the dominant factor that contributes to the lens shrinkage with a contribution of 42.058%. MT and IS have about the same contribution on the lens shrinkage each with a contribution of 25.820

**Table 10.** The viewing angle variation analysis.

Factor	Sum of squares (SS)	fDOF (f)	V Variation	S' Pure change	$\rho$ contribution (%)
MoT	0.126	2	0.063	0.126	53.670
MeT	0.101	2	0.050	0.101	42.776
IS	0.004	2	0.002	0.004	1.673
MoT/MeT	0.00045	4	0.0001125	0.00045	0.191
MoT/IS	0.00039	4	0.0000975	0.00039	0.166
MeT/IS	0.00121	4	0.0003025	0.00121	0.514
MoT/MeT/IS	0.00075	6	0.000125	0.00075	0.319
Error	0.00162			0.00162	0.690
Total (St)	0.235	24	0.0098	0.235	100.00%

**Table 11.** The optimum combination of Taguchi experiments.

Optimal exp.	Shrinkage (%)				Luminance uniformity (%)				Viewing angle (°)			
	1	2	3	Ave.	1	2	3	Ave.	1	2	3	Ave.
Shrinkage exp.	2.264	2.269	2.268	2.267	86.41	86.50	86.49	86.471	125	127	127	126.3
Luminance and viewing angle exp.	2.769	2.785	2.809	2.789	87.29	87.34	86.96	87.182	127	128	129	128

and 26.981%, respectively. With a higher MoT, the lens cools slower and provides more time for packing that makes the lens shrink less. Besides, there is less cooling rate difference throughout the lens during moulding, the melt has more time to relax and will have less thermal stress resulting in more uniform shrinkage of the lens.

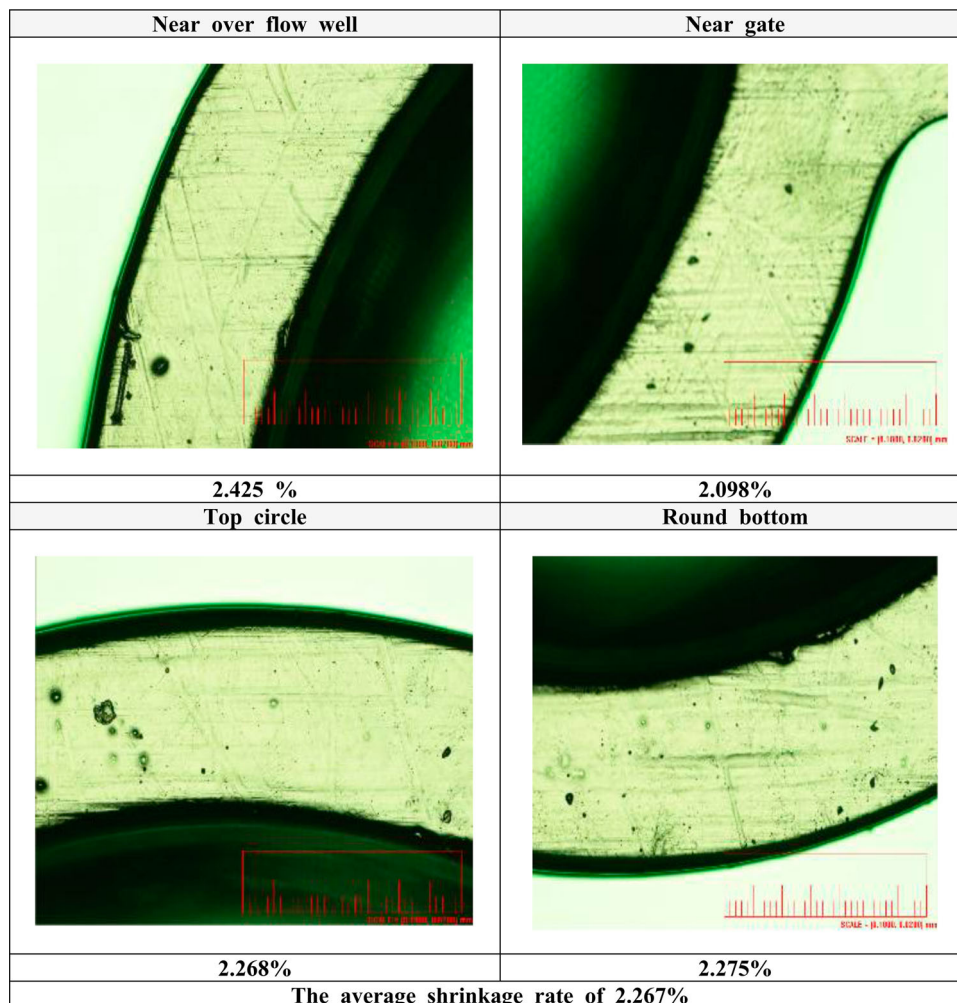
The variation analysis results for the luminance uniformity of LED were listed in Table 9. It showed that MoT contributed the highest percentage to the luminance uniformity LED. The percentage of MoT is 58.326%, followed by MT (24.30%) and IS (2.17%). While the variation analysis results for the viewing angle of LED were given in Table 10. It showed that the MoT contributed the highest percentage to the viewing angle of the LED. The percentage of MoT is 53.670%, followed by MT (29.589%) and IS (7.1%).

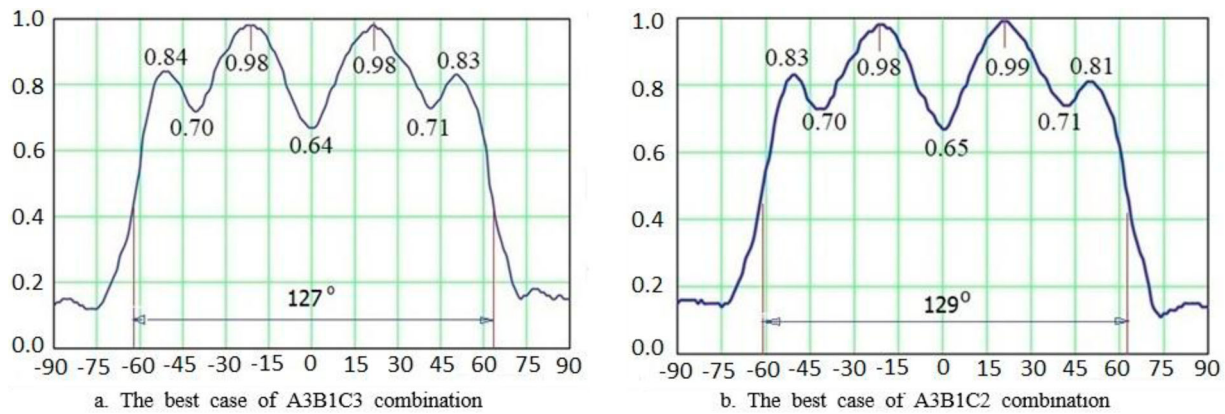
The variation analysis of the three Taguchi experiments reveals that MoT is the dominant parameter to produce the highest quality of LED lens in all three qualities.

### Optimal results

After obtaining the best combinations of injection process parameters for small shrinkage (A3B1C3) and for both high luminance uniformity and high viewing angle (A3B1C2). Optimal experiments were carried out. The optimal qualities of the experiments are listed in Table 11. For shrinkage, A3B1C3 has a smaller shrinkage (2.267%) than that of A3B1C2 (2.876%). Figure 15 shows one measurement results of the lens moulded with A3B1C3 combination, the shrinkage near the gate is smaller than that near the overflow well since the packing pressure is higher near the gate. The pressures at the top and the bottom circle are about the same, the shrinkages at the two locations are about the same.

The luminance uniformity value of best group (A3B1C3) for shrinkage is 86.47% and the viewing angle values is 127° (Figure 16(a)), while the light

**Figure 15.** Sample of the shrinkage results of A3B1C3 combination.



**Figure 16.** The results of luminous distribution measurement.

distribution value of best group (A3B1C2) for luminance uniformity and viewing angle is 87.18% and the viewing angle values is 129° (Figure 16(b)).

## Conclusion

Integrating computer-aided analysis, Taguchi experimental method, and micromoulding technologies, this study has developed an LED lens that has a luminance uniformity of 87.18% and a viewing angle of 128°. With the extra 1° draft angle in the lens mould, both the optical qualities drop a little bit but it provides the lens to be successfully demoulded from the mould. Though the lens studied is relatively small, it still needs a draft angle for a successful production with PMMA material.

## Acknowledgment

The financial support is acknowledged.

## Disclosure statement

No potential conflict of interest was reported by the authors.

## Funding

This work was supported by Ministry of Science and Technology (MOST) Taiwan [grant number 103-2221-E-151-061].

## ORCID

Fatahul Arifin  <http://orcid.org/0000-0002-8973-0709>

## References

- [1] Corporate information [cited 2018 Nov 25]. Available from: [www.nichia.co.jp](http://www.nichia.co.jp).
- [2] Haozhong G, Fangyi L, Shouyi G. LED principles and applications. Taipei, Taiwan: Five South Books Publishing Co., Ltd; 2012.
- [3] [cited 2018 Nov 25]. Available from: [www.ledlightforyou.com/aboutleds/led\\_design\\_and\\_functionality.jsp](http://www.ledlightforyou.com/aboutleds/led_design_and_functionality.jsp).
- [4] Understanding the basics of LED lenses [cited 2018 Nov 25]. Available from: [www.greenlightoptics.com](http://www.greenlightoptics.com)
- [5] Chang YC, Ou CJ, Tsai YS, et al. Non-Spherical LED packaging lens for uniformity improvement. *Opt Rev.* 2009;16(3):323–325.
- [6] Hsu YC. An optimum design and fabrication of lens on luminous uniformity and light extraction of high-power light-viewing diode. *Opt Rev.* 2011;18(1):27–33.
- [7] Chen WC, Lai TT, Wang M-W, et al. An optimization system for LED lens design. *Expert Syst Appl.* 2011;38(9):11976–11983.
- [8] Lo YC, Huang KT, Lee XH, et al. Optical design of a butterfly lens for a street light based on a double-Cluster LED. *Microelectron Reliab.* 2012;52:889–893.
- [9] Shi Y, Li B, Zhao M, et al. The design of LED rectangular uniform illumination lens. *Optic.* 2017;144:251–256.
- [10] La M, Park SM, Kim W, et al. Injection molded plastic lens for relay lens system and optical imaging probe. *Int J Prec Eng Manuf.* 2015;16(8):1801–1808.
- [11] Wang M-W, Chen CH, Arifin F, et al. Modelling and analysis of multi-shot injection molding of blue -ray objective lens. *J. of Mechanical Science and Technology.* 2018;32(10):4839–4849.
- [12] Oktem H, Erzurumlu T, Uzman I. Application of Taguchi optimization technique in determining plastic injection molding process parameters for a thin-shell part. *Mater Des.* 2017;28(4):1271–1278.
- [13] Erzurumlu T, Ozelik B. Minimization of warpage and sink index in injection-molded thermoplastic parts using Taguchi optimization method. *Mater Des.* 2006;27(10):853–861.
- [14] Lee K, Lin JC. Optimization of injection molding parameters for LED lampshade. *Transactions of the Canadian Society for Mechanical Engineering.* 2013;37(3):313–323.
- [15] Chen C-CA, Vu TL, Qiu YT. Study on injection molding of shell mold for aspheric contact lens fabrication. *Advances in Material & Processing Technologies Conference. Procedia Engineering.* 2017;184:344–349.
- [16] Lin JC, Lee KS. Molding analysis of multi-cavity aspheric lens and mold designing. *Adv Mater Process Techno.* 2009;83–86:77–87. ISSN: 1662-8985.
- [17] Lai HE, Wang PJ. Study of process parameters on optical qualities for injection-molded plastic lenses. *Appl Opt.* 2008;47(12):2017–2027.
- [18] Wang S, Ying J, Chen C. Grey fuzzy PI control for packing pressure during injection molding process. *J. of Mechanical Science and Technology.* 2011;25(4):1061–1068.
- [19] Taguchi G, Chowdhury S, Wu Y. Taguchi's quality engineering handbook. Hoboken (NJ): Wiley; 2005.